VOL. 11, NO. 4, FEBRUARY 2016 ISSN 1819-6608
ARPN Journal of Engineering and Applied Sciences


www.arpnjournals.com

PREDICTING THE SLIDING AMPLITUDE OF PLASTIC DEFORMATION IN THE RECIPROCATING SLIDING CONTACT

M. Nagentrau, W. A. Siswanto and A. L. Mohd Tobi
Faculty of Mechanical and Manufacturing Engineering, Universiti Tun Hussein Onn Malaysia, Batu Pahat, Malaysia
E-Mail: nagentrau.rau17@yahoo.com

ABSTRACT

This paper discusses a finite element analysis of a flat plate subjected to normal constant loading (cylinder-on-flat configuration) with reciprocating sliding contact. The material properties follow a linear kinematic hardening plasticity model and the manipulated reciprocating tangential displacements are simulated for different sliding amplitudes, starting from 0.05 mm, 0.1 mm and 0.2 mm respectively. The predicted plastic deformation evolution on the contact region are reported for several parameters, i.e. equivalent plastic strain, tangential plastic strain, shear plastic strain tangential stress and shear stress distributions. The effect of applied sliding displacement amplitude on stress and strain distributions is also investigated. The simulation results show that the stress distributions for kinematic hardening model are almost similar pattern for all three sliding displacements. The plastic strain distribution is proportional to the reciprocating sliding displacement amount, higher sliding displacement resulting higher plastic strain distribution. The trend of the plastic strain distributions is increasing consistently when the sliding displacement varies from 0.05 mm, 0.1 mm and 0.2 mm. It is found that the strain effect depends on the sliding displacement amplitude.

Keywords: reciprocating sliding, cyclic plasticity, sliding amplitude.

INTRODUCTION

The characteristics of excellent corrosion resistance, formability and fatigue resistance makes titanium alloy as an attractive material which widely used in research to study its properties (Joshi, 2006). A progressive and continuous removal of material from its surface by a mechanical action which results in deformation is termed as wear (Rabinowicz, 1995). The condition where two materials are forced to contact with the presence of sliding is known as sliding wear. Sliding wear is considered complicated type of wear as different material shows different respond under reciprocating sliding (Pirso *et al.* 2004). The study of deformation of solids that touch at one or more points is defined as the contact mechanics (Johnson, 1885). In addition, tribology is referred as the science of rubbing where science and interacting surfaces engineering act in a relative motion (Bhushan, 1999). Friction is referred as a resistance to a motion where more than one bodies slide on each other with the presence of contact (Gale and Totemeier, 2004). The tendency of material to experience a permanent deformation under the presence of force is termed as plasticity (Kachanov, 2004). Besides that, the plastic deformation of ductile body is due to asperities of the harder body and a cyclic plastic shear strain is induced that accumulated by repeated cycles (Boher *et al.* 2009). Moreover, the elastic plastic stress strain response plays a pivotal role in the designing and analyses of failure of engineering component (Jiang and Zhang, 2008). The finite element (FE) outcome for the gross sliding condition shows that delamination of wear mechanism comprising shear yielding, plastic deformation, ratcheting or shakedown, accumulation of plastic strain, multiple parallel cracking, TTB (tribological transformed structure) and formation of debris are the major concerns lead to the surface wear (Mohd Tobi *et al.* 2009). Furthermore, the linear kinematic hardening is yield surface translation in stress space via the back stress, $\boldsymbol{\alpha}$ which comprised in evolution law of a model (Dassault Systemes, 2010). The displacement effect in predicting plasticity of reciprocating sliding contact of linear kinematic hardening model is studied.

In this paper, plastic deformation is predicted based on plastic strain distributions along with tangential and shear stresses for a cylinder-on-flat contact configuration FE model using Ti-6Al-4V material. The FE model is validated with Hertzian contact theoretical solution. The failure of Ti-6Al-4V material due to plastic deformation can cause costly flaws, especially in industries, hence this study is significant.

SIMULATION METHOD

FE Modelling

The investigation of a flat plate subjected to normal constant loading in this work employs a cylinder-on-flat configuration as studied by Nagentrau *et al.* in 2014. The dimension of the flat plate is set as 100 mm x 24 mm x 8 mm and the radius of the cylinder is 6.5 mm as shown in the schematic diagram in Figure-1. The material examined in this analysis are Ti-6Al-4V alloy. The Young's modulus of 115 *GPa* and the Poisson's ratio of 0.342 are taken based on the study presented by Mohd Tobi *et al.* (2009), meanwhile plastic hardening properties is taken from the study of Benedetti and Fontanari (2004) as shown in Table-1.

Table-1. Linear cyclic plasticity hardening properties of Ti–6Al–4V (Benedetti & Fontanari, 2004).

Cyclic plasticity properties of Ti-6Al-4V	
Yield stress, σy	840 MPa
Hardening Modulus, c	7.32 GPa

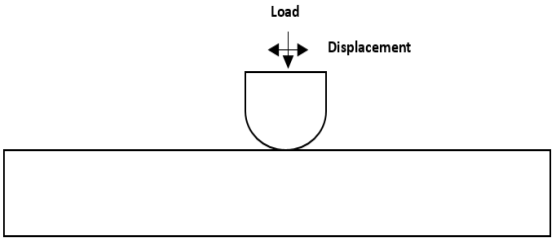

Figure-1. The schematic view of contact configuration

Figure-2 shows the FE model assembly with three element sets named as Point load, Top and Bottom surface respectively. The normal load, P of 200 N is applied at the Point load. The Bottom surface is constrained in both *x* and *y* directions. The Equation type constraint is assigned to ensure all the nodes of the top surface move simultaneously and horizontally with the point load according to the sliding displacement set for the analysis.

Two types of surfaces such as master surface (cylinder contact surface) and slave surface (flat contact surface) have been created in this model. Surface-to-surface contact approach with Lagrange Multiplier contact algorithm is used to ensure exact stick condition. Lagrange Multiplier contact algorithm suitable for friction involved contact problems as the shear stress is lower than critical shear value based on the friction law (Johnson, 1885). The friction coefficient is set as *0.9*. Subsequently, four steps (including initial condition) have been applied during modelling process where normal load, P applied at point load during Step-1, the cylinder moves right then left and finally to the right again to complete one cycle during Step-2, Step-3 and Step-4. The sliding amplitude of the cylinder is manipulated as 0.05 mm, 0.1 mm and 0.2 mm in order to study the plastic deformation response.

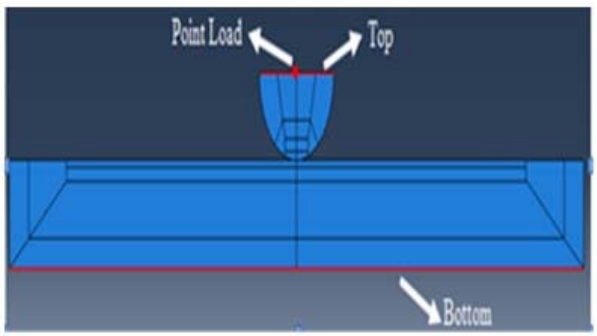

Figure-2. The model assembly.

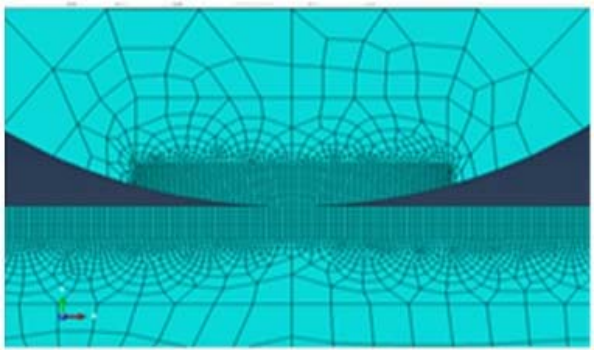

Figure-3. Contact region mesh module.

The mesh is refined at the contact region and the transition of the mesh from coarser to finer is achieved via edge seeding techniques as shown in Figure-3. Quad structured mesh of 50 µm square mesh is implemented at the contact region, while Quad-free-advanced mesh is applied at the further region. The implementation of mesh transition grant better plasticity prediction and reduce the analysis computational time as the study mainly focus on contact region. The contact variables is compared with Hertzian theoretical solution to validate the model and proceed the study.

RESULTS AND DISCUSSION

FE Model Validation

Figure-4 illustrates comparison of theoretical and numerical contact pressure distributions. The FE predicted contact pressure distribution shows similar trend as Hertzian contact theoretical solutions where the maximum contact pressure occurs at the center of the contact. The calculated maximum contact pressure, po and contact half-width length, a are 798.6 MPa and 0.2 mm respectively. Meanwhile, the FE predicted maximum contact pressure, po and half-width contact length, a are 740.9 MPa and 0.3 mm. The FE predicted contact distribution gives good agreement with Hertzian theoretical solution.

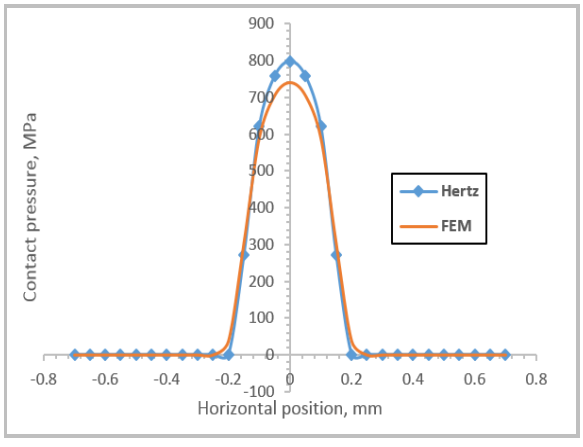

Figure-4. Comparison of theoretical and numerical contact pressure distributions.

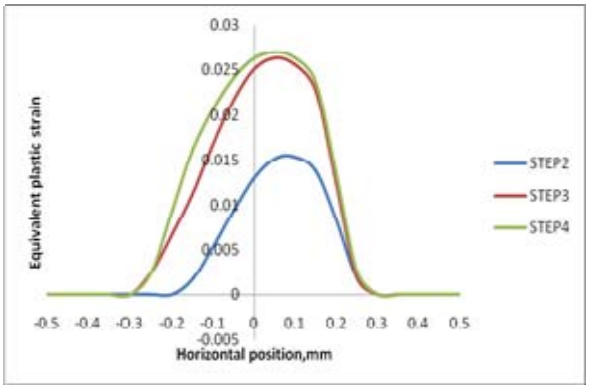

Figure-5. Equivalent plastic strain for 0.05 mm sliding amplitude.

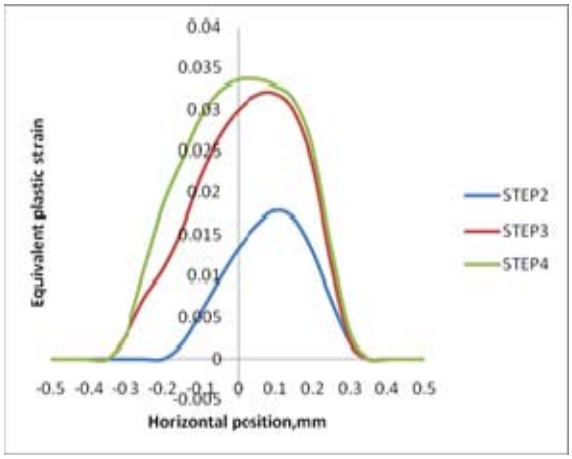

Figure-6. Equivalent plastic strain for 0.1 mm sliding amplitude.

The Evolution of Plastic Strain Distributions

Figure-5, Figure-6 and Figure-7 show that evolution of equivalent plastic strain (PEEQ) for linear kinematic hardening of sliding displacements of 0.05 mm, 0.1 mm and 0.2 mm respectively. Obviously, the value of PEEQ is higher at step 4 compared to step 3 and step 2 for all sliding displacements as plasticity accumulation occur based on sliding amount. In addition, the higher the sliding displacement the higher the PEEQ where 0.2 mm of sliding displacement showing higher value of plastic strain compared to 0.1 mm and 0.05 mm. The PEEQ graphs trend showing that there is less increment of plastic strain in step 4 compared with step 3 for all displacements but very significant in 0.2 mm displacement. Basically, the peaks at leading and trailing edges are due to plasticity effects on both edges as it is influenced by the direction of the movement of the cylinder.

Figure-8, Figure-9 and Figure-10 show that the tangential plastic strain (PE11) evolution of sliding displacements of 0.05 mm, 0.1 mm and 0.2 mm. According to the analysis it is noticeable that when the sliding displacement amount and number of steps increases more disturbances occur at the curve of the graph. Generally, more ripples found in the step 4 of all the displacement and the formation of ripples very significant at higher sliding displacement which leads to occurrence excessive movement and stretching.

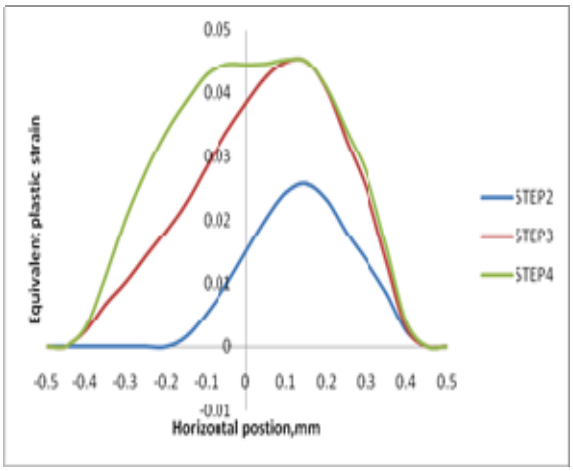

Figure-7. Equivalent plastic strain for 0.2 mm sliding amplitude.

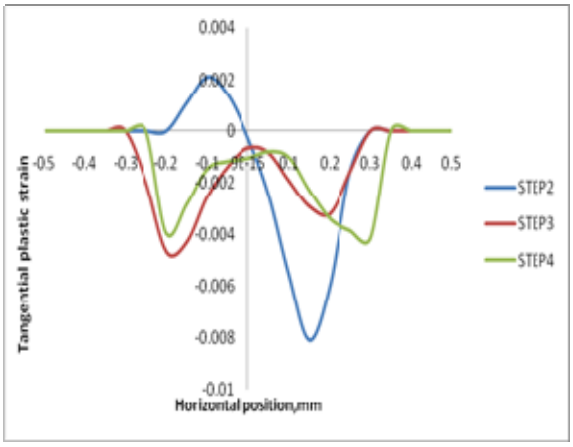

Figure-8. Tangential plastic strain for 0.05 mm sliding amplitude.

Figure-11, Figure-12 and Figure-13 show that the shear plastic strain (PE12) evolution of sliding displacements of 0.05 mm, 0.1 mm and 0.2 mm respectively. The shear plastic strain (PE12) showing higher value compared with the tangential plastic strain (PE11) for all cases. In addition, maximum PE12 occurs at step 2 for all the sliding displacement. Obviously, when the number of steps and sliding displacement amount increases more disturbances occur at the curve of the graph same as the PE11, where more ripples can be noticed mainly at step 4 and higher displacement. Generally, the stress does not show significant increment compared with the strain graphs.

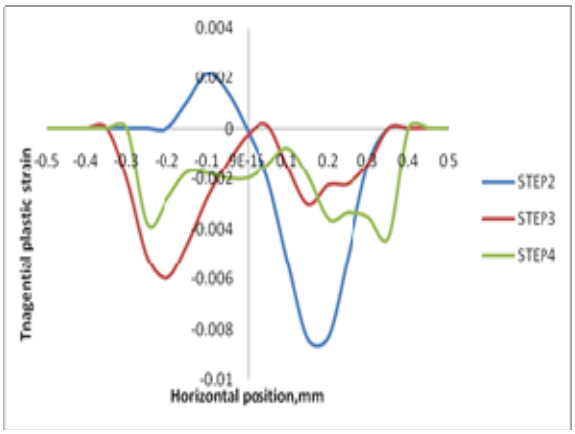

Figure-9. Tangential plastic strain for 0.1 mm sliding amplitude.

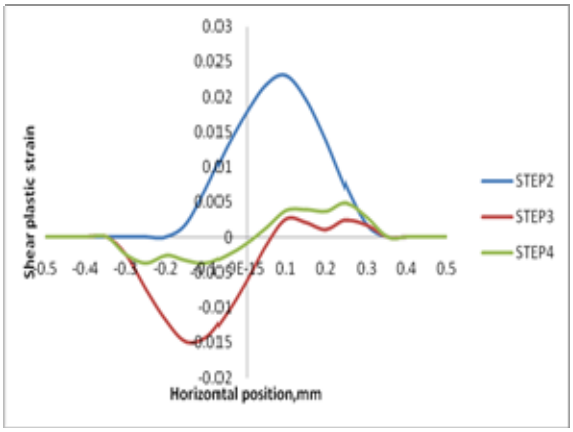

Figure-12. Shear plastic strain for 0.1 mm sliding amplitude.

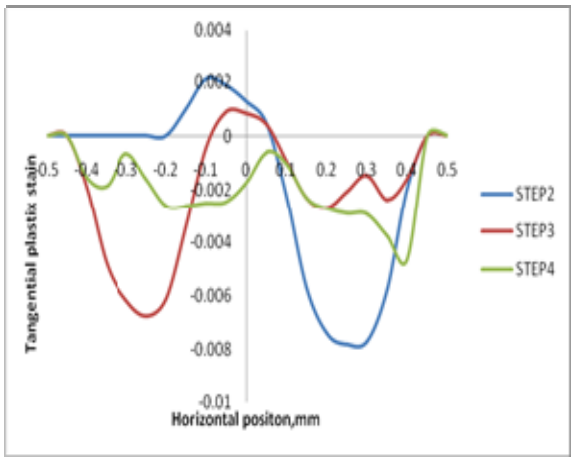

Figure-10. Tangential plastic strain for 0.2 mm sliding amplitude.

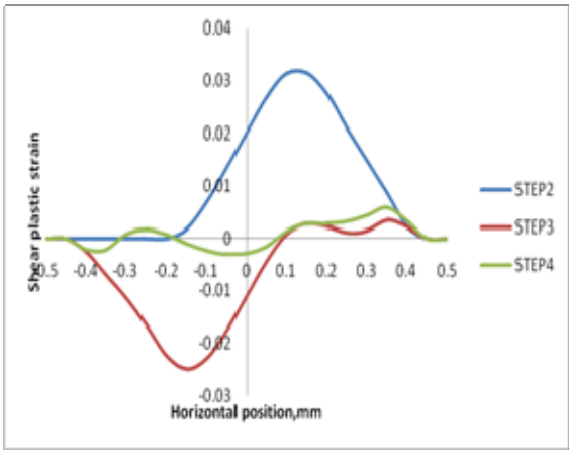

Figure-13. Shear plastic strain for 0.2 mm sliding amplitude.

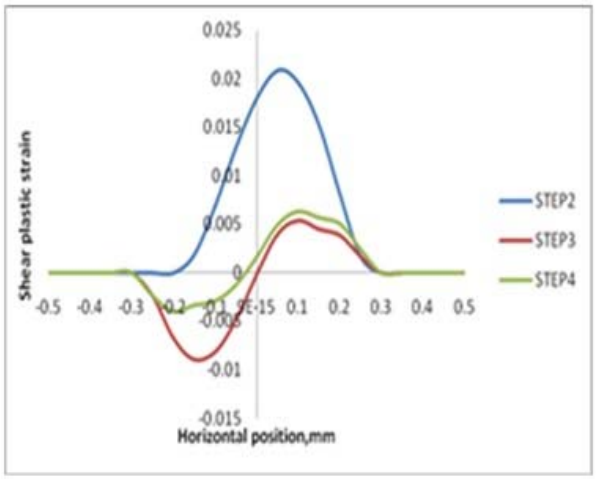

Figure-11. Shear plastic strain for 0.05 mm sliding amplitude.

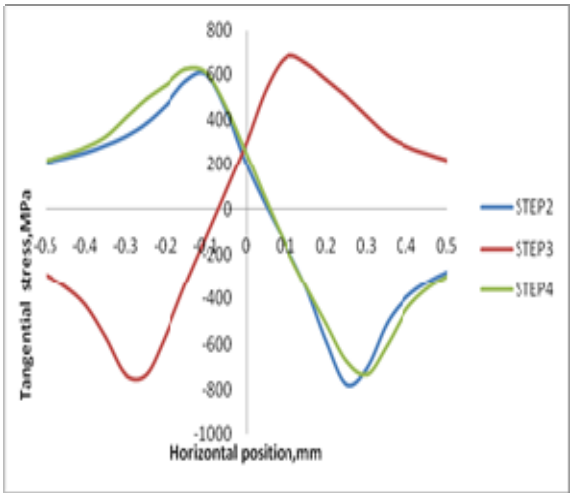

Figure-14. Tangential stress for 0.05 mm sliding amplitude.

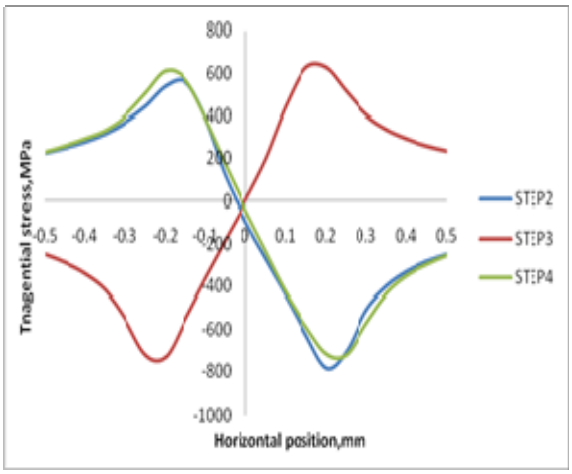

Figure-15. Tangential stress for 0.1 mm sliding amplitude.

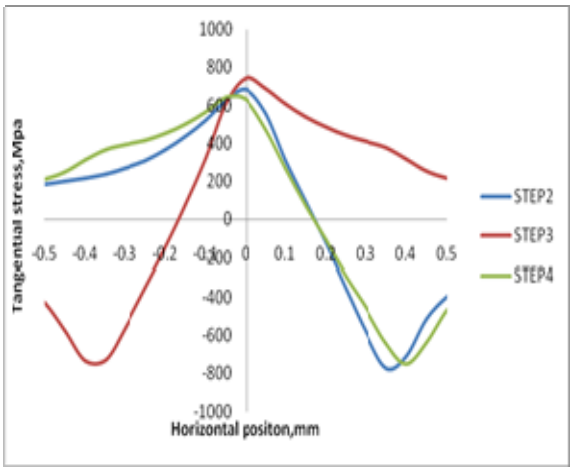

Figure-16. Tangential stress for 0.2 mm sliding amplitude.

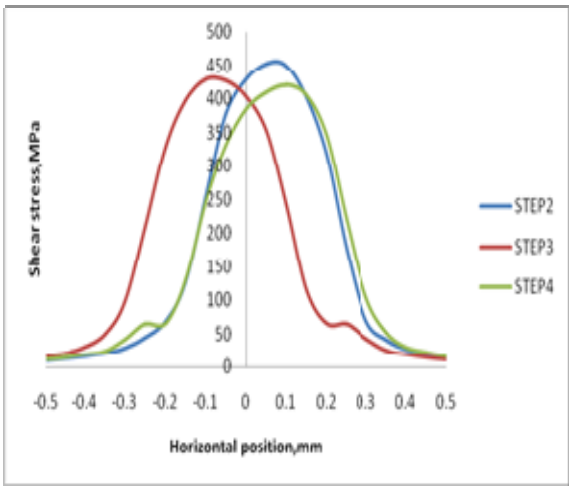

Figure-17. Shear stress for 0.05 mm sliding amplitude.

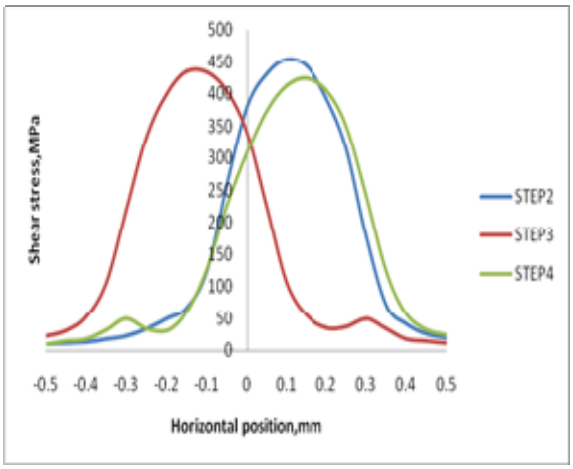

Figure-18. Shear stress for 0.1 mm sliding amplitude.

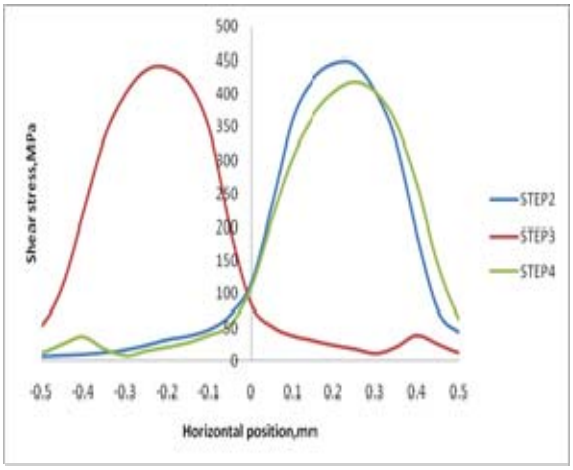

Figure-19. Shear stress for 0.2 mm sliding amplitude

THE EVOLUTION OF TANGENTIAL STRESS AND SHEAR STRESS DISTRIBUTIONS

Figure-14, Figure-15 and Figure-16 show tangential stress (S11) evolution, while Figure-17, Figure-18 and Figure-19 show evolution of shear stress (S12) for linear kinematic hardening of sliding displacements 0.05 mm, 0.1 mm and 0.2 mm respectively. The tangential stress predicted to be higher at the trailing edges if compared with leading edges of the contact area for all displacements. It is predicted that the compressive stress has been occurred at the leading edges meanwhile the tensile stress occurred at the trailing edges. The compressive stress occurred at leading edge due to initial pressure of normal load which compresses the material. There are no much difference in tangential stress (S11) and shear stress (S12) for the sliding displacements amount of 0.05 mm, 0.1 mm and 0.2 mm. Besides that, tensile tangential stress and compressive tangential stress of step 3 look like mirrored as negative displacement occur from right to left for all the displacements

DISCUSSIONS

Based on the analysis, it is obvious that the equivalent plastic strain (PEEQ) value increases as the sliding displacement amount increases. This as a result of the equivalent plastic strain (PEEQ) value is calculated based on the summation of the tangential and shear plastic strain values. Besides that, shear yielding effect of high frictional force due to high displacement amplitude causes the shear plastic strain is more significant than the tangential plastic strain. There are more disturbances occur at higher sliding amount of tangential and shear plastic strain, especially in step 4 as the flat plate might be stretched excessively and hardened due to excessive amount of sliding and load applied on repeated sliding. Basically, when it slides to the side, the fresh side causes the occurrence of new hardening which results in ripples on the graphs. Generally, fatigue will be influenced by the strain most on early cycles, but due to higher amount of displacement, it hardened and causes no increment in plasticity strain as stress effect takes over. This phenomenon leads where the strain is increasing but stress remains same and does not show any significant changes. In addition, tangential and shear components for stress-strain are looked at as they can lead to development of higher stress or strain and result in material deformation (Hibbeler, 2000). Meanwhile, shear and tangential stress-strain distribution are important factor in the occurrence of plastic deformation process by slipping and twinning (Lal and Reddy, 2009).

CONCLUSIONS

The core objective of this study is to investigate and predict the effect of sliding amplitude on the plasticity behavior on Ti-6Al-4V titanium alloy where cylinder on flat surface configuration finite element modelling with linear kinematic hardening is used for this study. Apparently, in the process of predicting the plasticity the strain is much more significant than the stress. The strain distribution increases with increasing sliding amount. The maximum sliding amount causes the formation of ripples on tangential and shear plastic strain graphs, where more disturbance occur on the 0.2 mm sliding model compared with 0.1 mm and 0.05 mm. This is due to the excessive stretching of material at higher displacement. As the predicted stress is saturated, the tangential and shear stress graph does not show significant changes.

ACKNOWLEDGEMENTS

The authors acknowledge the financial support by the Malaysian Ministry of Education and Universiti Tun Hussein Onn Malaysia (UTHM) (Research Acculturation Collaborative Effort No. 1441).

REFERENCES

[1] Benedetti M. & Fontanari V. (2004). The effect of bi-modal and lamellar microstructure of Ti–6Al–4V on the behavior of fatigue cracks emanating from edge notches. Fatigue Fracture of Engineering Materials Structures 27 (11) 1073–1089.

[2] Bhushan, B. (1999). Priciples and Applications of Tribology.John Wiley & Sons, Inc.

[3] Boher, C., Barrau, O., Gras, R., & Rezai-Aria, F. (2009). A wear model based on cumulative cyclic plastic straining. Wear 267(5-8), 1087–1094.

[4] Dassault Systemes, (2010). Abaqus Theory Manual. Version 6.10. RI, USA

[5] Gale, W.F & Totemeier TC. (2004). Smithells Metals Reference Book, 8th Ed. Elsevier Butterwirth-Heinemann.

[6] Hibbeler, R. C. (2000). Mechanics of Materials, Prentice Hall.

[7] Jiang, Y. & Zhang, J. (2008). Benchmark experiments and characteristic cyclic plasticity deformation. International Journal of Plasticity, 24(9), 1481–1515.

[8] Johnson K.L (1985). Contact Mechanics. Cambridge University Press, Cambridge.

[9] Joshi, V. A. (2006). Titanium Alloys (An Atlas of Structures and Fracture Features), CRC PressTaylor & Francis Group, Florida, 7-15.

[10] Kachanov, L.M. (2004). Fundamental of theory of plasticity. Amsterdam, north-Holland Pub Co., 1971, in series: North-Holland series in applied mathematics and mechanic ISBN 0-486-43583-0.

[11] Lal, G. K., & Reddy, N. V. (2009). Introduction to Engineering Plasticity. Alpha Science International Limited.

[12] Mohd Tobi, A.L., Ding, J., Bandak, G., Leen, S.B. & Shipway, P.H., (2009), A study on the interaction between fretting wear and cyclic plasticity for Ti-6Al-4V. Wear, 267 pp. 270-282.

[13] Pirso, J., Letunovitš, S. & Viljus, M. (2004). Friction and wear behavior of cemented carbides. Wear, 257, 257-265.

[14] Rabinowicz, E. (1995). Friction and Wear of Materials. 2nd Edition: Society of Tribologists and Lubrication Engineers (STLE), 840 Busse Highway Park Ridge, IL 60068-2302 USA.